中国物理 B
Chinese Physics
中国物理
Chinese Physics B

Structural model of substitutional sulfur in diamond

Hongyu Yu(于洪雨), Nan Gao(高楠), Hongdong Li(李红东), Xuri Huang(黄旭日), Defang Duan(段德芳), Kuo Bao(包括), Mingfeng Zhu(朱明枫), Bingbing Liu(刘冰冰), Tian Cui(崔田)

Citation: Chin. Phys. B . 2019, 28(8): 088102 . **doi:** 10.1088/1674-1056/28/8/088102
Journal homepage: http://cpb.iphy.ac.cn; http://iopscience.iop.org/cpb

What follows is a list of articles you may be interested in

Inclusions in large diamond single crystals at different temperatures of synthesis

Fei Han(韩飞), Shang-Sheng Li(李尚升), Xue-Fei Jia(贾雪菲), Wei-Qin Chen(陈玮琴), Tai-Chao Su(宿太超), Mei-Hua Hu(胡美华), Kun-Peng Yu(于昆鹏), Jian-Kang Wang(王健康), Yu-Min Wu(吴玉敏), Hong-An Ma(马红安), Xiao-Peng Jia(贾晓鹏)

Chin. Phys. B . 2019, 28(2): 028103 . **doi:** 10.1088/1674-1056/28/2/028103

Effect of FeS doping on large diamond synthesis in FeNi–C system

Jian-Kang Wang(王健康), Shang-Sheng Li(李尚升), Quan-Wei Jiang(蒋全伟), Yan-Ling Song(宋艳玲), Kun-Peng Yu(于昆鹏), Fei Han(韩飞), Tai-Chao Su(宿太超), Mei-Hua Hu(胡美华), Qiang Hu(胡强), Hong-An Ma(马红安), Xiao-Peng Jia(贾晓鹏), Hong-Yu Xiao(肖宏宇)

Chin. Phys. B . 2018, 27(8): 088102 . **doi:** 10.1088/1674-1056/27/8/088102

Band offset and electronic properties at semipolar plane AlN(1101)/diamond heterointerface

Kong-Ping Wu(吴孔平), Wen-Fei Ma(马文飞), Chang-Xu Sun(孙昌旭), Chang-Zhao Chen(陈昌兆), Liu-Yi Ling(凌六一), Zhong-Gen Wang(王仲根)

Chin. Phys. B . 2018, 27(5): 058101 . **doi:** 10.1088/1674-1056/27/5/058101

Synthesis of diamonds in Fe—C systems using nitrogen and hydrogen co-doped impurities under HPHT

Shi-Shuai Sun(孙士帅), Zhi-Hui Xu(徐智慧), Wen Cui(崔雯), Xiao-Peng Jia(贾晓鹏), Hong-An Ma(马红安)

Chin. Phys. B . 2017, 26(9): 098101 . **doi:** 10.1088/1674-1056/26/9/098101

Different effect of NiMnCo or FeNiCo on the growth of type-IIa large diamonds with Ti/Cu as nitrogen getter

Shang-Sheng Li(李尚升), He Zhang(张贺), Tai-Chao Su(宿太超), Qiang Hu(胡强), Mei-Hua Hu(胡美华), Chun-Sheng Gong(龚春生), Hon-An Ma(马红安), Xiao-Peng Jia(贾晓鹏), Yong Li(李勇)

Chin. Phys. B . 2017, 26(6): 068102 . **doi:** 10.1088/1674-1056/26/6/068102

Structural model of substitutional sulfur in diamond*

Hongyu Yu(于洪雨)[1,2], Nan Gao(高楠)[1], Hongdong Li(李红东)[1,†], Xuri Huang(黄旭日)[2], Defang Duan(段德芳)[1], Kuo Bao(包括)[1], Mingfeng Zhu(朱明枫)[1], Bingbing Liu(刘冰冰)[1], and Tian Cui(崔田)[1,‡]

[1] *State Key Laboratory of Superhard Materials, College of Physics, Jilin University, Changchun* 130012, *China*
[2] *Institute of Theoretical Chemistry, Jilin University, Changchun* 130012, *China*

(Received 17 April 2019; revised manuscript received 12 June 2019; published online 25 July 2019)

Based on ab initio calculations, it is found that the donor center of substitutional sulfur (S) in diamond with C_{2v} symmetry is more stable than that with C_{3v} symmetry, which is different from previous reports in literature. The energy difference of C_{2v} and C_{3v} structures is qualitatively affected by the supercell size, and the 216-atom supercell could be proposed as the minimum to obtain stable configuration of substitutional S in diamond. Using supercells of up to 512 atoms, the donor level of substitutional S with C_{2v} symmetry is deep.

Keywords: substitutional sulfur in diamond, structural model, molecular dynamic simulation, supercell size

PACS: 81.05.ug, 74.62.Dh, 52.65.Yy, 63.20.dk **DOI:** 10.1088/1674-1056/28/8/088102

1. Introduction

Diamond having unique physicochemical properties is considered as one of the most promising materials for next generation semiconductors.[1] It is well-known that p-type diamond have been successfully obtained by boron (B) doping,[2,3] however, the fabrication of n-type diamond with a shallow donor level is extremely difficult. In order to achieve the shallow doping for n-type diamond, kinds of donors have been attempted, such as lithium,[4,5] nitrogen,[6–9] phosphorus,[10–13] oxygen,[14] and sulfur (S),[15–17] *etc*.

Doping with S was reported to be an effective method to obtaining the n-type diamond,[15,18] then a number of computational approaches have been employed to estimate the donor model and donor level value.[19–31] One possibility of the origin of the donor levels may be substitutional S (S_{sub}),[1] and the most stable configuration of S_{sub} in diamond is generally considered to S atom and four carbon (C) neighbors with C_{3v} symmetry,[26–29] and the C_{2v} configuration is considered as the less stable structure.[27,28] Then, it has been achieved kinds of donor level values between -0.15 eV to -1.63 eV for S_{sub} in diamond with C_{3v} symmetry.[19–29] However, nearly all of the supercells were relaxed at a fixed volume using structural optimizations to simulate the potential field of diamond, and most of supercells calculated only contained 64 atoms to minimize the computational cost.[30] It is assumed that the donor center structure of S_{sub} and the donor level value are qualitatively affected by the supercell size (namely, the doping concentration) and optimization methods.

Since the molecular dynamic (MD) simulations can exhibit the changing of the structure parameter of S_{sub} in diamond at room temperature as the function of time, it has been successfully used to predict the new structure of ammonium azide under high pressure,[32] consider the tanglesome rotation of ammonium cation in ammonium nitrate[33] and understand the kinetic and thermodynamic properties of the closing and opening of a base pair.[34] In this paper, both the *ab initio* MD simulations and structural optimizations are considered for the structural model of S_{sub} in diamond with the larger supercells. We find that the C_{2v} symmetry is the stable structure for S_{sub} in diamond, and the minimum supercell is 216-atom.

2. Computation details

All calculations performed in this paper are based upon *ab initio* density functional theory simulations, as implemented in Vienna *Ab-initio* Simulation Package (VASP) code.[35] The projector-augmented wave (PAW)[36,37] method is adopted and the cutoff energy of 520 eV is set. The Perdew–Burke–Ernzerhof (PBE) function based on the generalized gradient approximation (GGA)[37] is employed to describe the exchange and correlation effects of electrons. The MD simulations are implemented both in the isobaric isothermal (*NPT*) ensemble at 300 K, and atmospheric pressure and canonical (*NVT*) ensemble at 300 K. The optimized lattice parameters of pristine diamonds with 64-, 216-, and 512-atom supercells are 7.146 (3.573×2), 10.7189 (3.573×3), and 14.292 (3.573×4) Å, which are agree well with the experimental sin-

*Project supported by the National Natural Science Foundation of China (Grant Nos. 11704143, 51672102, 51632002, and 11604023), the National Key Research and Development Program of China (Grant Nos. 2018YFA0305900 and 2016YFB0201204), and the Program for Changjiang Scholars and Innovative Research Team in University (Grant No. IRT-15R23).

†Corresponding author. E-mail: hdli@jlu.edu.cn
‡Corresponding author. E-mail: cuitian@jlu.edu.cn

© 2019 Chinese Physical Society and IOP Publishing Ltd

gle cell lattice value of 3.567 Å,[38] and then one C atom is replaced with a S atom for MD simulations. In MD simulations, the Brillouin zone is sampled using the Monkhorst–Pack scheme, with mesh of $3\times3\times3$, $2\times2\times2$, and $1\times1\times1$ for 64-, 216-, and 512-atom supercells, respectively. The time steps of 1.0 fs and total simulation times of at least 10 ps are used, and all the MD simulations achieve thermalisation after 3 ps by examining the system pressure and temperature. After MD simulations, we optimize the averaged structures and calculate the total energies of the three supercells with k mesh of $7\times7\times7$, $5\times5\times5$, and $3\times3\times3$, respectively.

3. Results and discussions

First, the MD simulations both in the NVT and NPT ensembles at 300 K are performed to investigate the S_{sub} structure. The main difference between the NVT and NPT ensembles is that the volume, side length and side angle of supercell for the former are restricted constant, while those in the latter are allowed to optimize. Figure 1 show the bond lengths and bond angles between the S dopant and four adjacent C atoms with the 64-atom supercell. For NVT MD simulation steps shown in Figs. 1(a) and 1(c), after the simulation reaches equilibrium, one S–C bond length increases to 1.95 Å, and the other three bonds keep at $\sim$ 1.72 Å. The lattice parameters in the last 1.0 ps are averaged, and a C_{3v} symmetry donor center is obtained by further geometry relaxation. Additionally, the longer S–C bond length and lager C–S–C bond angle appear alternately, indicating that the system hops from one configuration to the other three equivalent C_{3v} structures. It is consistent with previous results, which considered that C_{3v} pattern was more stable.[27,28] As a contrast, for NPT MD simulation in Figs. 1(b) and 1(d), the four S–C bond length values are almost equal as the time increases, and a C_{2v} symmetry donor center is obtained by averaging over the lattice parameters after 9.0 ps. Moreover, the hoping of S atoms in the donor center of C_{2v} supercells can also be observed. It is concluded that C_{3v} (C_{2v}) symmetry is more stable for NVT (NPT) ensemble for S_{sub} in diamond with the 64-atom supercell. Considering the opposite results of NPT and NPV MD simulations, the supercell is increased in the following.

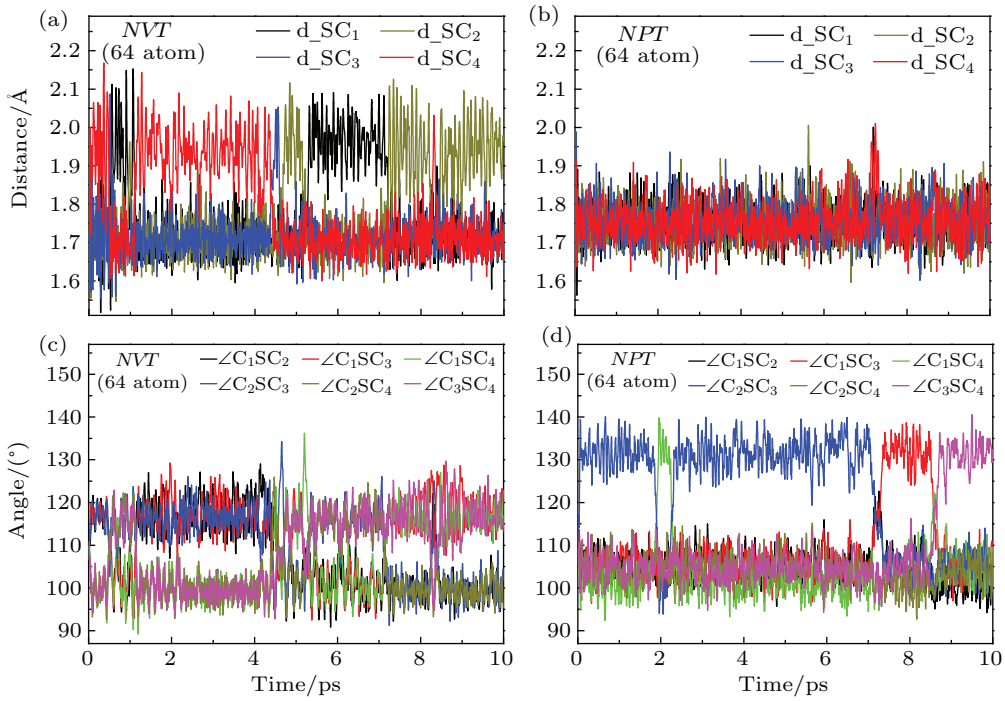


Fig. 1. The distance between S and four adjacent C atoms (d_SC$_i$, i = 1, 2, 3, 4) as a function of the MD simulation time in (a) NVT and (b) NPT ensembles, and the six bond angles in donor center ($\angle$C$_i$SC$_j$, i, j = 1, 2, 3, and 4) as a function of the MD simulation time in (c) NVT and (d) NPT ensembles. The calculations are performed with 64-atom supercell.

Figures 2(a)–2(d) exhibit the S–C bond length and C–S–C bond angle in 216-atom supercell as a function of MD simulation time. Both the NVT and NPT ensemble simulations suggest that the C_{3v} and C_{2v} donor center appears alternately. Furthermore, the S–C bond length and C–S–C bond angle as a function of MD simulation steps in the 512-atom supercells in Figs. 3(a)–3(d) show that at the most of NVT simulation time, the donor center performs as C_{2v} symmetry, and during almost the entire NPT simulation, the donor center is C_{2v} symmetry. Thus, for the NVT simulation, the C_{3v} symmetry donor center transforms into C_{2v} structure, when the supercell is larger than 216, namely, C_{2v} symmetry donor center for S_{sub} in diamond with a larger supercell is more possible. However, for NPT ensemble calculations, C_{2v} symmetry always appears with the 64- and 512-atom supercells, while the C_{2v} and C_{3v} structures hop alternatively with the 216-atom supercell.

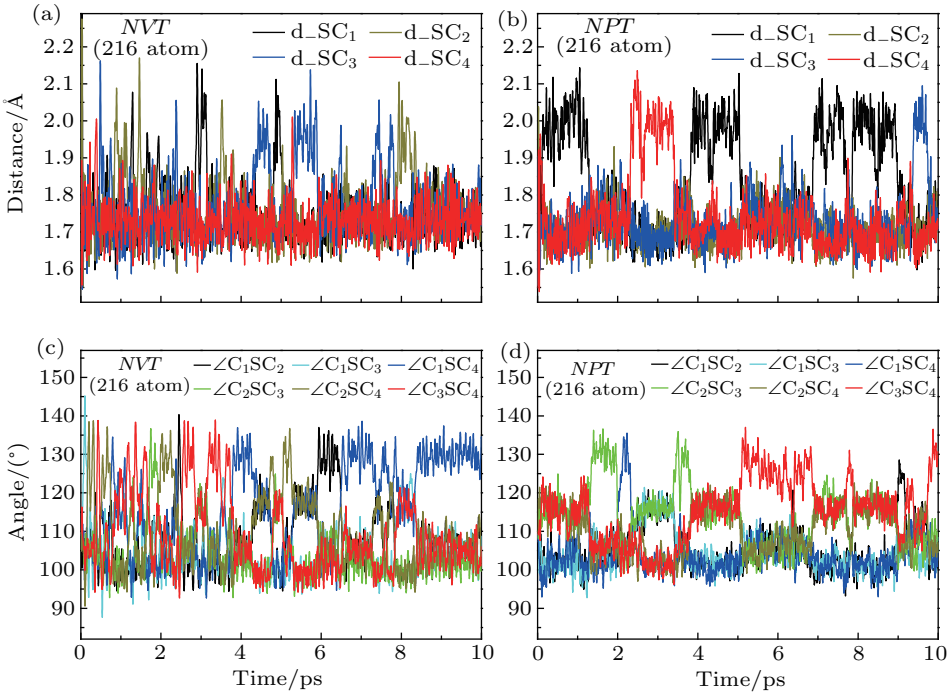


Fig. 2. The distance between S and four adjacent C atoms (d_SC$_i$, $i = 1, 2, 3, 4$) as a function of the MD simulation time in (a) *NVT* and (b) *NPT* ensembles, and the six bond angles in donor center ($\angle$C$_i$SC$_j$, i, $j = 1, 2, 3$, and 4) as a function of the MD simulation time in (c) *NVT* and (d) *NPT* ensembles. The calculations are performed with 216-atom supercell.

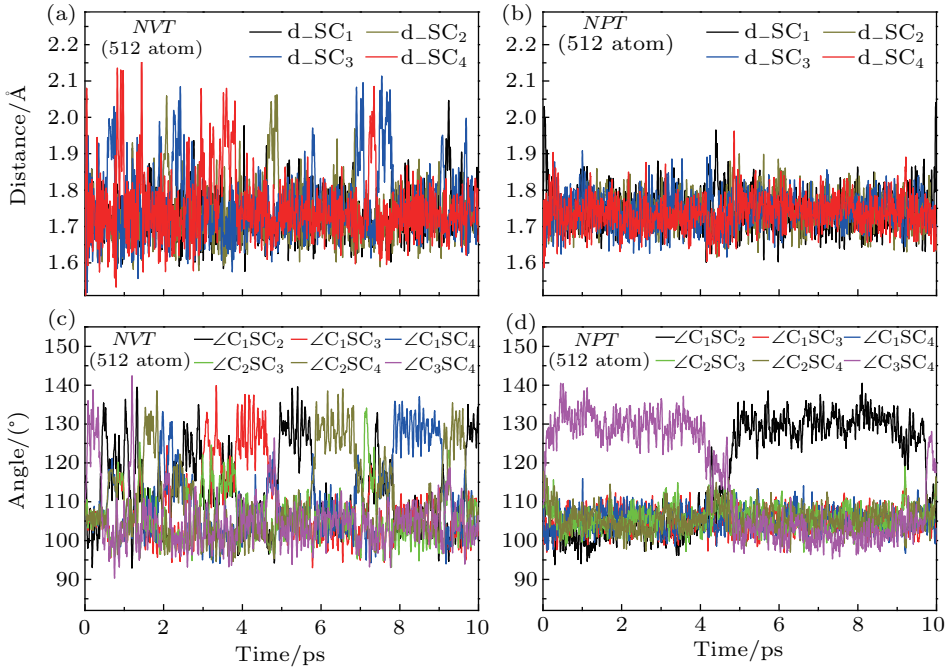


Fig. 3. The distance between S and four adjacent C atoms (d_SC$_i$, $i = 1, 2, 3, 4$) as a function of the MD simulation time in (a) *NVT* and (b) *NPT* ensembles, and the six bond angles in donor center ($\angle$C$_i$SC$_j$, i, $j = 1, 2, 3$, and 4) as a function of the MD simulation time in (c) *NVT* and (d) *NPT* ensembles. The calculations are performed with 512-atom supercell.

To explain it, the three lattice angles of S_{sub} in diamond with 64-, 216-, and 512-atom supercells and pristine diamond with 512-atom supercell during *NPT* MD simulations are given in Fig. 4. For 64-atom supercell, the averaged lattice angle of 91.0656° or 88.9465° is far away from that of cubic structure. Especially, the averaged angle values of 216- and 512-atom supercell are nearly 90°, which are close to the cubic supercell. Thus, the result obtained from *NPT* MD calculations with 64-atom supercell is not reliable. Consequently, from the *NPT* MD results, we also obtain the same conclusion that the minimum supercell to obtain converged values of S_{sub} in diamond is 216-atom. The different symmetry of S_{sub} in diamond are obtained for *NVT* and *NPT* ensembles with 64-, 216-atom supercell, while the same symmetry is realized with the 512-atom supercell. This is because that during the MD simulation with limited number of atoms, there are still inter-

action between the boundary atoms and S dopant. Thus, the different restrictions for the atomic location in the boundary between the *NVT* and *NPT* ensembles result in the different geometry of impurity centers. When the simulated supercell is large enough, the influence of the impurity atom at the supercell boundary atoms is negligible, and thus the difference between the *NVT* and the *NPT* ensemble is also negligible.

Then, the structures under a series of density functional theory (DFT) structural optimizations are obtained to further confirm the stable S_{sub} structure. First, the ionic positions, the lattice shape and parameters of C_{3v} and C_{2v} structures are fully relaxed, namely, the pressure is zero. The relative energies for fully relaxed structures show that the C_{2v} structure is more stable for 64-, 216-, and 512-atom supercells (Table 1). Moreover, the lattice parameters are closer to those of cubic, when the supercell is larger than 216-atom. Then, the relative atomic positions in C_{3v} and C_{2v} structures are kept invariant, and the lattice parameters are adjusted to be cubic, only the ionic positions are relaxed. Four representative lattice parameters of 7.206, 7.203, 7.146, and 7.134 Å are selected for the supercells, corresponding to the C_{3v} structure with zero pressure, C_{2v} structure with zero pressure, relaxed pristine diamond, and experimental value of pristine diamond.[39] As shown in Table 2, in the 64-atom cubic structures, the energy of C_{3v} donor center is lower than that of C_{2v}, just as discussed in literature.[27,28] However, the pressures of C_{3v} structures are higher than those of C_{2v} with the same lattice parameters, denoting that the conclusion need to be further versified. Further calculations with 216- and 512-atom supercell indicate that the C_{2v} symmetry is more stable. Moreover, the deviation of lattice angles has a limited impact on the energy difference between C_{2v} and C_{3v} supercell at 512-atom condition, but it significantly reduces the energy difference at 216-atom condition.

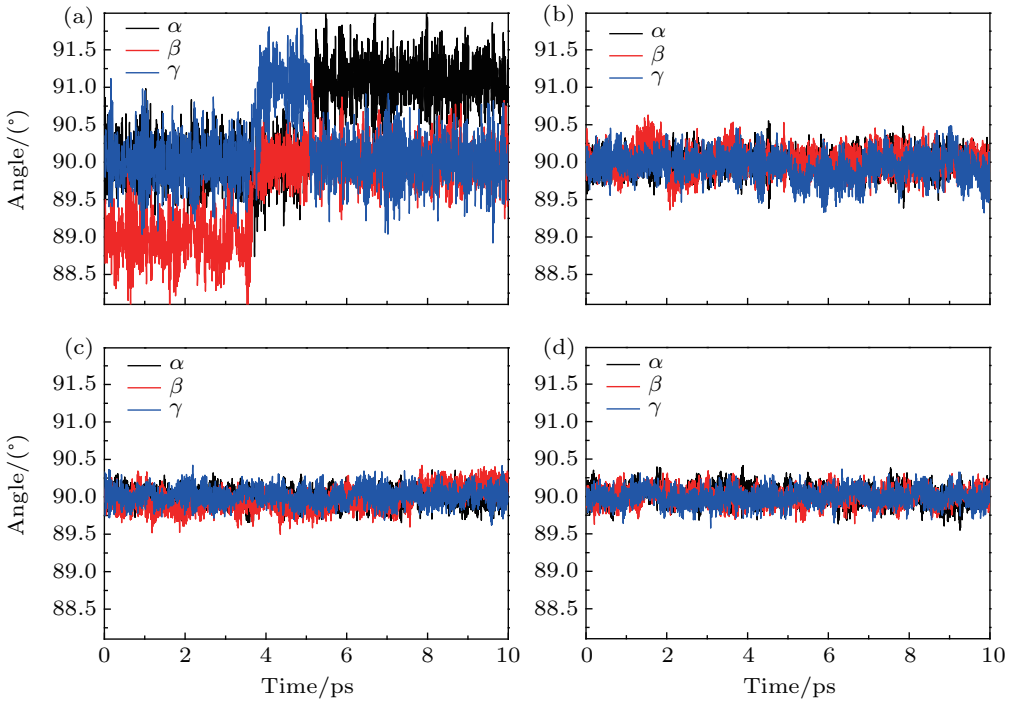


Fig. 4. The lattice angle of S_{sub} in diamond with (a) 64-, (b) 216-, and (c) 512-atom supercells and (d) pristine diamond with 512-atom supercell as a function of *NPT* MD simulation time.

Table 1. The lattice parameters of fully relaxed supercells with C_{2v} and C_{3v} donor centers with 64-, 216-, and 512-atom supercells.

		C_{2v}			C_{3v}		
64-atom	Angle/(°)	91.0702	89.9997	89.9997	90.3020	90.3018	90.3017
	Side length/Å	7.119	7.244	7.244	7.205	7.205	7.205
	Relative energy/eV					0.2243	
216-atom	Angle/(°)	89.7028	90.0000	90.0000	89.9465	90.0000	90.0000
	Side length/Å	10.707	10.761	10.761	10.745	10.761	10.761
	Relative energy/eV		0			0.1803	
512- atom	Angle/(°)	90.1213	90.0003	90.0002	89.9800	90.0215	89.9787
	Side length/Å	14.285	14.315	14.316	14.307	14.307	14.307
	Relative energy/eV		0			0.1291	

Table 2. The parameters of relaxed cubic supercells with C_{2v} and C_{3v} donor centers with 64-, 216-, and 512-atom supercells. ΔP = pressure (C_{2v})−pressure (C_{3v}).

	Side length/Å	Relative energy ΔE/eV		Pressure (kB, C_{2v})	Pressure (kB, C_{3v})	ΔP/kB
		C_{2v}	C_{3v}			
64- atom	7.206	0	–0.1514	–5.58	0.00	–5.58
	7.203	0	–0.1498	0.00	5.59	–5.59
	7.146	0	–0.1185	103.23	109.08	–5.85
	7.134	0	–0.1119	126.18	132.06	–5.88
216-atom	10.745	0	0.0686	–2.00	0.00	–2.00
	10.743	0	0.0693	0.00	1.99	–1.99
	10.719	0	0.0844	29.94	31.96	–2.02
	10.701	0	0.0923	52.24	54.29	–2.05
512-atom	14.306	0	0.1181	–0.94	0.00	–0.94
	14.305	0	0.1184	0.00	0.88	–0.88
	14.292	0	0.1230	12.24	13.15	–0.91
	14.268	0	0.1309	34.36	35.21	–0.85

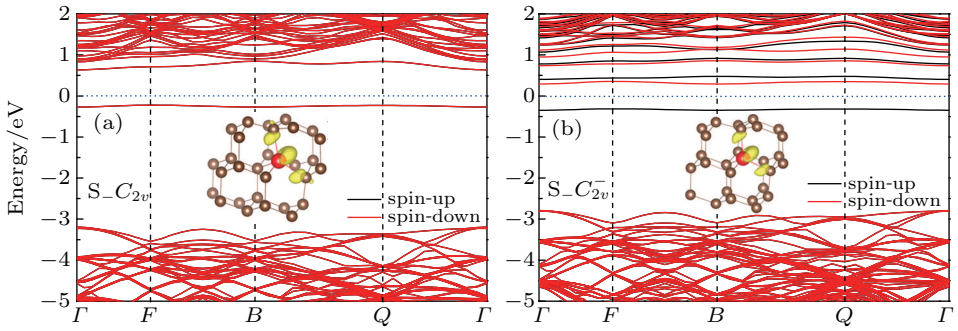


Fig. 5. The band structures of S_{sub} in diamond with 512-atom supercell with C_{2v} symmetry in (a) neutral and (b) positive charge states. The insert shows the isosurface plot for the donor level near Fermi energy. The brown balls are C atom, and red is S atom.

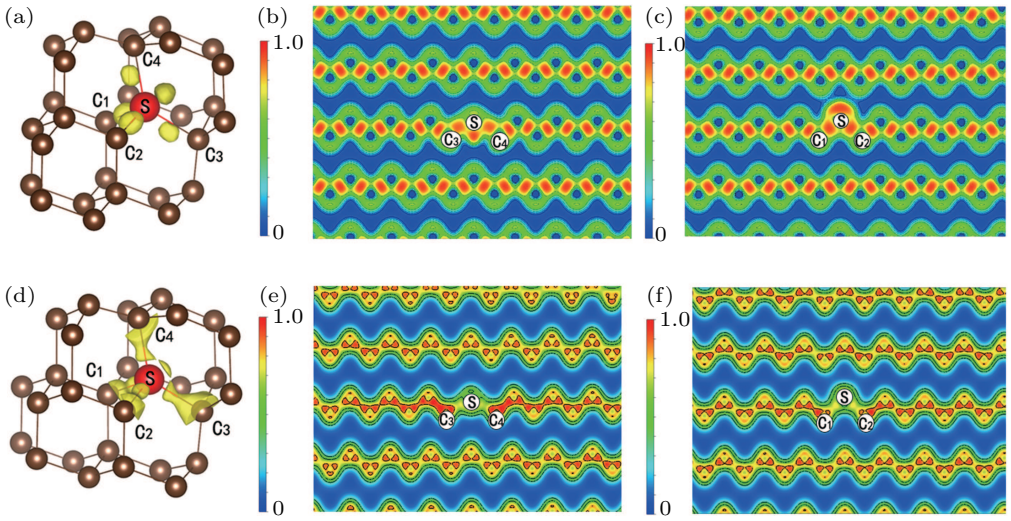


Fig. 6. Partial structures of [(a), (b), (c)] ELF and [(d), (e), (f)] charge density of S_{sub} in diamond in 512-atom supercell with C_{2v} symmetry. 2D ELF contour plots of the plane crossing (b) S, C_3, and C_4 atoms, and (c) S, C_1, and C_2 atoms. 2D charge density contour plots of the plane crossing (e) S, C_3, and C_4 atoms, and (f) S, C_1, and C_2 atoms. The brown balls are C atom, and red is S atom. Blue to red indicates the gradually increased charge localization.

The band structures of 512-atom with C_{2v} symmetry in neutral and positive charge state (named as S_C_{2v} and S_C_{2v}^{+}) are shown in Figs. 5(a) and 5(b), respectively. The former is spin-degenerated, while partial bands near the Fermi level for the latter are spin-splitting. For the case of S_C_{2v} (Fig. 5(a)), the donor level is about 1.1 eV with respect to the conduction band minimum (CBM). For S_C_{2v}^{+} (Fig. 5(b)), the occupied spin-up donor level is about 1.6 eV below the CBM, and the spin-down donor level is un-occupied. It denotes that the S_{sub} in diamond is a deep donor. The partial charge density (PCD) for donor level at Fermi surface in the inset denotes that the lone pair electrons and the electrons in the nearest S–

C bond have a major contribution to the donor level, as the discussion of substitutional phosphorus in diamond.[12] In order to have the further insight into the bonds near the S atom, the partial structures of electron localization function (ELF), which has widely been used to reveal the bonding, lone electron pairs, atomic shell structure,[40] is shown in Fig. 6(a). At the same time, two-dimensional contour plots of ELF for the plane crossing the S, C_1, and C_2, and S, C_3, and C_4 atoms are shown in Figs. 6(b) and 6(c), respectively. One can see that the S atom is bonded with four neighbor C atoms, with the remaining two electrons forming a lone-pair orbital between the C_3 and C_4 atoms. In detail, the bonding orbital between the S–C_3 and S–C_4 are repulsed from the lone-pair electron. Furthermore, we present the charge density distribution and its two-dimensional contour plots of the plane crossing S, C_1, and C_2, and S, C_3, and C_4 in Figs. 6(d)–6(f). The charge localization between C_3 and S (or C_4 and S) is more evident than that between C_1 and S, indicating that the lone pair electrons have a major effect on the two nearest S–C_3 and S–C_4 bonds, and further impact the electron distribution between two C atoms those in the same plane with S, C_3 and C_4 (labeled in Fig. 6(e)), while in other direction, the impact of electron distribution is neglected (Fig. 6(f)).

4. Conclusions

In conclusion, the stable donor center structure of S_{sub} in diamond is studied by a series of MD simulations and structural optimizations using the 64-, 216-, and 512-atom supercells. The C_{3v} center is the more stable configuration in the cubic supercell with 64 atoms, while the C_{2v} center is more energetically stable with a larger supercell. Our results indicate that 216-atom supercell is the minimum supercell to obtain the accurate structure of S_{sub} in diamond. The S_{sub} with C_{2v} donor center has a deep donor level, which mainly comes from the lone pair electrons located between two S–C bonds. It is expected that more studies on S-doped diamond and co-doped diamond with S and other donor impurities are needed.

Acknowledgment

The calculations were performed in the High Performance Computing Center (HPCC) of Jilin University.

References

[1] Goss J P, Eyre R J and Briddon P R 2008 *Phys. Stat. Solidi B* **245** 1679
[2] Fontaine F, Uzan S C, Philosoph B and Kalish R 1996 *Appl. Phys. Lett.* **68** 2264
[3] Ueda K, Kasu M and Makimoto T 2007 *Appl. Phys. Lett.* **90** 122102
[4] Goss J P, Eyre R J and Briddon P R 2007 *Phys. Stat. Solidi A* **204** 2978
[5] Lombardi E and Mainwood A 2007 *Physica B: Condens. Matter* **401** 57
[6] Farrer R G 1969 *Solid State Commun.* **7** 685
[7] Kajihara S A, Antonelli A, Bernholc J and Car R 1991 *Phys. Rev. Lett.* **66** 2010
[8] Yiming Z, Larsson F and Larsson K 2014 *Theor. Chem. Acc* **133** 1432
[9] Dai Y, Dai D, Yan C, Huang B and Han S 2005 *Phys. Rev. B* **71** 075421
[10] Gheeraert E, Koizumi S, Teraji T and Kanda H 2000 *Solid State Commun.* **113** 577
[11] Pinault M A, Temgoua S, Gillet R, Bensalah H, Stenger I, Jomard F, Issaoui R and Barjon J 2019 *Appl. Phys. Lett.* **114** 112106
[12] Butorac B and Mainwood A 2008 *Phys. Rev. B* **78** 235204
[13] Yan C X, Dai Y, Guo M, Huang B B and H D 2009 *Appl. Surf. Sci.* **255** 3994
[14] Long R, Dai Y and Yu L 2007 *J. Phys. Chem. C* **111** 855
[15] Sakaguchi I, N -Gamo M, Kikuchi Y, Yasu E, Haneda H, Suzuki T and Ando T 1999 *Phys. Rev. B* **60** R2139
[16] Kalish R, Reznik A, Uzan-Saguy C and Cytermann C 2000 *Appl. Phys. Lett.* **76** 757
[17] Wang J K, Li S S, Jiang Q W, Song Y L, Yu K P, Han F, Su T C, Hu M H, Hu Q, Ma H A, Jia X P and Xiao H Y 2018 *Chin. Phys. B* **27** 088102
[18] Nishitani-Gamo M, Yasu E, Xiao C, Kikuchi Y, Ushizawa K, Sakaguchi I, Suzuki T and Ando T 2000 *Diamond Relat. Mater.* **9** 941
[19] Anderson A B, Grantscharova E J and Angus J C 1996 *Phys. Rev. B* **54** 14341
[20] Saada D, Adler J and Kalish R 2000 *Appl. Phys. Lett.* **77** 878
[21] Zhou H, Yokoi Y, Tamura H, Takami S, Kubo M, Miyamoto A, N.-Gamo M and Ando T 2001 *Jpn. J. Appl. Phys.* **40** 2830
[22] Nishimatsu T, Katayama-Yoshida H and Orita N 2001 *Physica B: Condens. Matter* **302** 149
[23] Wang L G and Zunger A 2002 *Phys. Rev. B* **66** 161202
[24] Sque S J, Jones R, Goss J P and Briddon P R 2004 *Phys. Rev. Lett.* **92** 017402
[25] Lombardi E B, Mainwood A and Osuch K 2004 *Phys. Rev. B* **70** 205201
[26] Goss J, Briddon P, Jones R and Sque S 2004 *Diamond Relat. Mater.* **13** 684
[27] Miyazaki T and Okushi H 2001 *Diamond Relat. Mater.* **10** 449
[28] Miyazaki T 2002 *Phys. Stat. Solidi A* **193** 395
[29] Yu C, Zhang T, Anderson A B, Angus J C, Kostadinov L N and Albu T V 2006 *Diamond Relat. Mater.* **15** 1868
[30] Tang L, Yue R and Wang Y 2018 *Carbon* **130** 458
[31] Sque S J, Jones R, Goss J P and Briddon P R 2003 *Physica B: Condens. Matter* **340** 80
[32] Yu H, Duan D, Tian F, Liu H, Li D, Huang X L, Liu Y X, Liu B B and Cui T 2015 *J. Phys. Chem. C* **119** 25268
[33] Yu H, Duan D, Liu H, Yang T, Tian F, Bao K, Li D, Zhao Z L, Liu B B and Cui T 2016 *SCI REP-UK* **6** 18918
[34] Wang Y J, Wang Z, Wang Y L and Zhang W B 2017 *Chin. Phys. B* **26** 128705
[35] Kresse G and Furthmüller J 1996 *Phys. Rev. B* **54** 11169
[36] Blöchl P E 1994 *Phys. Rev. B* **50** 17953
[37] Kresse G and Joubert D 1999 *Phys. Rev. B* **59** 1758
[38] Perdew J P, Burke K and Ernzerhof M 1996 *Phys. Rev. Lett.* **77** 3865
[39] Czelej K, Śpiewak P and Kurzydłowski K J 2016 *MRS Adv.* **1** 1093
[40] Becke A D and Edgecombe K E 1990 *J. Chem. Phys.* **92** 5397